



# Correlation between microbes and colorectal cancer: tumor apoptosis is induced by sitosterols through promoting gut microbiota to produce short-chain fatty acids

Hang Ma<sup>1</sup> · Yang Yu<sup>1</sup> · Meimei Wang<sup>1</sup> · Zhaoxing Li<sup>1,3</sup> · Heshan Xu<sup>2</sup> · Cheng Tian<sup>1</sup> · Jian Zhang<sup>2</sup> · Xiaoli Ye<sup>2</sup> · Xuegang Li<sup>1</sup>

Published online: 30 November 2018  
© Springer Science+Business Media, LLC, part of Springer Nature 2018

## Abstract

The diversity of the bacterial community in the gut is closely related to human health. Gut microbes accomplish multiple physiological and biochemical functions. Sitosterols are a series of phytochemicals that have multiple pharmacological activities and are used as cholesterol-lowering drugs in clinical practice. In this study, we investigated the roles of bacteria and short-chain fatty acids (SCFAs) to the anti-colorectal cancer (anti-CRC) effects of sitosterols in BALB/c nude mice. Sitosterols were administered orally and gut microbiota composition and intestinal SCFAs changes were analyzed. The correlation between gut microbiota, SCFAs, and tumor apoptosis was assessed by a series of in vivo and in vitro experiments. Tumor growth in the mice was inhibited by sitosterol-treatment. Mechanistic studies revealed that sitosterol-treatment reduced the expression of PI3K/Akt, promoted the activation of Bad, decreased Bcl-xl, and enhanced cyto-c release, leading to caspase-9 and caspase-3 activation, PARP cleavage, and apoptosis. 16S rDNA analysis revealed that the diversity of microbiota, particularly phyla *Bacteroidetes* and *Firmicutes*, reduced dramatically in the gut of tumor-bearing mice, whilst treatment with sitosterols reversed these changes. The levels of SCFAs in the fecal samples of sitosterol-treated mice increased, leading to cancer cell apoptosis in vitro. Moreover, tumor apoptosis was induced after mice received a daily dose of  $2 \times 10^8$  CFU/0.2 mL *Lactobacillus pentosus* or 20 mM/0.2 mL SCFAs. Taken together, these results demonstrate that sitosterols maintain a diverse microbial environment and enrich the content of *L. pentosus* in the gut, leading to the production of beneficial metabolites including SCFAs that promote tumor apoptosis.

**Keywords** Colorectal cancer · Gut microbiota · Short-chain fatty acids · Sitosterols · *Lactobacillus pentosus*

## Abbreviations

CRC Colorectal cancer

SCFAs Short-chain fatty acids

NC Normal control

TC Tumor control

ST  $\beta$ -Sitosterol

STG  $\beta$ -Sitosterol-glucoside

STGL  $\beta$ -Sitosterol-glucoside-linoleate

LAC *Lactobacillus pentosus*

**Electronic supplementary material** The online version of this article (<https://doi.org/10.1007/s10495-018-1500-9>) contains supplementary material, which is available to authorized users.

✉ Xuegang Li  
Xuegangli@swu.edu.cn

<sup>1</sup> Chongqing Productivity Promotion Center for the Modernization of Chinese Traditional Medicine, School of Pharmaceutical Sciences, Southwest University, Chongqing 400716, China

<sup>2</sup> Chongqing Engineering Research Center for Sweet Potato, School of Life Sciences, Southwest University, Chongqing 400715, China

<sup>3</sup> McLean Hospital, Harvard Medical School, Belmont, MA 02478, USA

## Introduction

Colorectal cancer (CRC) is one of the most commonly diagnosed cancers in both men and women [1]. Recent statistical data estimates that CRC will lead to over 140,000 new cases and over 50,000 deaths in the United States in 2018, accounting for 8% of all cancer-related deaths [2, 3]. In industrialized countries, the lifetime risk of developing CRC is approximately 5%, and the risk of non-cancerous colorectal tumors (which can develop into CRC) is 20% [4].

Although definitive progress in the diagnosis, surgery and chemotherapy of CRC has occurred, it remains one of the top three leading causes of death in cancer patients, and a major cause of relapse and metastasis [4–6]. The etiology of CRC remains unclear, although several genetic risk factors have been proposed based on epidemiological studies [7–12], chronic bioassays for mutagens identified in animal models [13, 14], and germline mutations: 3% of cases are caused by hereditary nonpolyposis colorectal cancer (HNPCC) and 1% are caused by familial adenomatous polyposis (FAP) [15, 16]. Recent studies have shown that diets rich in red meat and processed meat, alcohol consumption, and chronic inflammation of the gastrointestinal tract are associated with CRC [17–20]. Most causative factors are closely associated with diet, and changes in the complex gut microbiota community.

Gut microbiota, resident in the large intestine of healthy adults at a density of more than  $10^{11}$  cells/gram contents, are regarded as an extra “organ” owing to their roles in providing nourishment, regulating epithelial development, and regulating innate immunity [21]. Accumulating evidence suggests that the composition and metabolism of gut microbiota influence several types of cancer by affecting inflammation, DNA damage and apoptosis [22]. In healthy adults, the major metabolites of the microbiota are gases and organic acids, mainly the three short-chain fatty acids (SCFAs); acetic, propionic and butanoic acid. Non-digestible carbohydrates are the primary substrates for microbial fermentation, including the structural polysaccharides of plant cell walls, resistant starch and soluble oligosaccharides [22]. Approximately 90% of SCFAs are rapidly absorbed in the gut amongst which butyrate is utilized as the preferred energy source by colonocytes, reaching only low concentrations in the systemic circulation. Propionate is primarily metabolized in the liver, whilst acetate passes more freely into the peripheral circulation reaching relatively high levels in the plasma [23]. Butyrate and propionate inhibit histone deacetylases (HDACs) in colonic epithelial and immune cells, promoting the hyperacetylation of histones. Subsequently, butyrate and propionate regulate CRC-related transcription factors and reduce the incidence of carcinogenesis. Furthermore, SCFAs regulate the activity of surface-exposed host cell receptors, mainly G protein-coupled receptors including GPR41, GPR43 and GPR109A [22].

In this study, we explored the influence of three sitosterols including  $\beta$ -sitosterol (ST),  $\beta$ -sitosterol-glucoside (STG), and  $\beta$ -sitosterol-glucoside-linoleate (STGL) isolated from sweet potato, on CRC development. Their structures are shown in Fig. S1. The anticancer activity of constituents from natural plants or foods has been widely reported. For example, Naoshad and colleagues showed that bitter melon extract inhibits breast cancer growth in preclinical models [24]. The anticancer effects of STGL

have not been reported, whilst ST is since generally recognized as a safe and effective natural nutritional supplement possessing several benefits including anti-oxidant, anti-microbial, angiogenic, immunomodulatory, anti-diabetic, anti-inflammatory, anti-nociceptive, and anti-cancer activities, with no significant toxicity [25]. Importantly, the three sitosterols do not inhibit the proliferation of CRC cell lines HCT-116, HT-29 and SW-480 (data not shown) in our preliminary in vitro experiments. Based on these results, we hypothesized that the anti-CRC activity of sitosterols may be largely related to the metabolic activity of gut microbiota. Subsequently, the BALB/c nude mouse model was employed to evaluate the anti-CRC effect of sitosterols and Illumina sequencing was used to investigate the differences in gut microbiota amongst normal, tumor-bearing, and sitosterol-treated mice. The inhibitory mechanism of gut microbiota on CRC was also studied.

## Materials and methods

### Materials

ST, STG, and STGL were purified in our lab by silica-gel column chromatography and semi-preparative high-performance liquid chromatography; they have purities all over 98.0%. Dulbecco's Modified Eagle medium (DMEM), fetal bovine serum (FBS), penicillin, streptomycin and trypsin were acquired from Gibco Life Technologies (Burlington, Ontario, Canada). Propidium iodide (PI), RNase, and 10% neutral-buffered formalin were obtained from Sangon Biotech Co., Ltd (Shanghai, China). Twelve Tumor Markers Test Kit (Microarray Chemiluminescent Immunoassay) was purchased from Ming Yuan Shu Kang Biochip Co., Ltd (Shanghai, China). “In Situ Cell Death Detection Kit” was obtained from Roche Diagnostics GmbH (Germany). Human CRC cell lines, HCT-116, HT-29, SW-480, and normal colorectal epithelial FHC cells were acquired from the Cell Bank of Chinese Academy of Sciences (Shanghai, China). *Lactobacillus pentosus* (ATCC 8041) was commercially provided by North of Shanghai Biological Technology Co., Ltd (Shanghai, China). Acetic acid, propionic acid and butanoic acid were provided by Adamas Reagent, Ltd (China). Four-week-old male BALB/c nude mice were supplied by Weitonglihua Co., Ltd (Beijing, China). Specific-pathogen-free (SPF)-grade feedstuff was purchased from Tengxin Co., Ltd (Chongqing, China). Antibodies against PI3K, Akt, Bad, Bcl-xl, Bax, Bcl-2 cyto-c, caspase-3, and caspase-9 were commercially provided by Proteintech Group, Inc (USA). Stool DNA Kit was purchased from Novogene Biological Information Technology Co., Ltd (Beijing, China).

## In vivo tumor xenograft study of sitosterols

Four-week-old male BALB/c nude mice were housed in a pathogen-free room in the Animal Experimental Center of Southwest University (Chongqing, China), with free access to food and water. All animal experimental protocols were approved by the Institutional Animal Ethics Committee of Southwest University, China. Animal experiments were carried out as described earlier [26]. Briefly, 25 BALB/c nude mice were randomly distributed into five groups with five animals in each: ST (treated with ST), STG (treated with STG), STGL (treated with STGL), normal control (NC), and tumor control (TC) groups. Animals from the same group are raised in the same cage. HCT-116 cells ( $7 \times 10^6$  per mouse) were harvested and suspended in a serum-free medium, followed by inoculating them into the right forelegs of mice of ST, STG, STGL, and TC groups, except for the NC group. After inoculation, mice in the ST, STG, or STGL groups received a daily oral administration of ST, STG, or STGL at the same dose of 60 mg/kg body weight, or 0.2 mL of 0.9% saline solution when they were in NC and TC group.

The growth of the tumor was measured by a vernier caliper every third day along two orthogonal axes i.e., length (L) and width (W). The volume (V) of the tumor was calculated by the equation for the ellipsoid ( $V = W^2 \times L/2$ ). In addition, the body weight of each mouse was recorded every third day. Fresh fecal samples (200 mg) from each group were collected in sterile containers with ice box on day 0, 15, and 30 and immediately stored at  $-80^\circ\text{C}$ . After mice were sacrificed on day 30, the organs and tumors were quickly dissected and stored at  $-80^\circ\text{C}$  for further examination. The serum tumor markers CEA, CA125, CA242 and CA199 were detected using multi-tumor marker protein chip diagnosis system, according to the manufacturer's instructions (Ming Yuan Shu Kang Biochip Co., Ltd, China).

## Western blotting

Tumor tissues from mice were homogenized and lysed by RIPA lysis buffer with protease inhibitor cocktail tablet and 1 mM PMSF for 15 min on a shaker at  $4^\circ\text{C}$ . As for proteins from in vitro cultured cells, HCT-116 cells were harvested. Proteins were collected from the lysed tissues by centrifuging for 15 min at  $12,000 \times g$  and then quantified for the western blotting analysis, followed by the addition of the loading buffer. After boiling for 5 min, the protein samples were separated through 12% SDS polyacrylamide gel electrophoresis and then transferred onto the polyvinylidene difluoride (PVDF) membranes. Subsequently, the membranes were blocked with 5% non-fat milk prepared in TBST buffer (Tris 10 mM, NaCl 150 mM, pH 7.6, 0.1% Tween 20) at room temperature for 1 h, and then probed with primary antibodies specific to  $\beta$ -actin, phosphoinositide 3-kinase (PI3K),

Akt, Bad, Bcl-xl, cyto-c, caspase-3, caspase-9, Bax, Bcl-2, or PARP at  $4^\circ\text{C}$  overnight. Primary antibodies were diluted 2000 times uniformly in TBST. The membranes were then incubated with horseradish peroxidase-conjugated secondary antibody (with 4000 times dilution) at room temperature for 1 h. The protein bands from antibody-antigen reactions were visualized using WesternBright™ ECL prime western blotting detection reagent.

## Immunohistochemistry study

Tumor tissues were fixed with formalin and embedded in paraffin according to standard histological procedures. The tissues were cut into  $4 \mu\text{m}$  sections, and then deparaffinized, rehydrated, and subjected to antigen recovery using 0.1 M citrate buffer in a microwave oven at high temperature for 30 min. Endogenous peroxidase activity was quenched by adding 3%  $\text{H}_2\text{O}_2$  for 15 min; subsequently, the sections were blocked in 10% normal goat serum for 1 h. The expressions of caspase-3 and caspase-9 were presented through the specific binding with their relevant polyclonal antibody (rabbit polyclonal, 1:600 dilution) and with the HRP-conjugated secondary antibody. After phosphate-buffered saline (PBS) washing, the chromogenic signal was developed with 3,3'-diaminobenzidine tetrahydrochloride in 50 mM Tris-HCl (pH 7.5) for 5 min. finally, the sections were counterstained with hematoxylin and visualized under a light microscope.

## TUNEL reaction

The TUNEL technique was carried out using the "In Situ Cell Death Detection Kit", according to the manufacturer's instructions. Briefly, the sections were air-dried for 15 min and fixed with 4% paraformaldehyde for 20 min. Then, they were washed thrice with PBS and treated with the fresh permeabilization solution (0.1% Triton X-100, 0.1% sodium citrate) on ice for 2 min. subsequently, the sections were rewashed with PBS and incubated with the TUNEL reaction mixture in the dark at  $37^\circ\text{C}$  for 1 h. The sections were then washed with PBS, counterstained with DAPI (4',6-diamidino-2-phenylindole) for the detection of nuclei and rewashed three times with PBS, after which they were examined under the microscope (Nikon Eclipse 80i, Japan).

## Illumina sequencing analysis of gut microbiota

The genomic DNAs of gut microbiota from BALB/c nude mice were extracted according to the manufacturer's directions of the Stool DNA Kit and their concentrations were determined using NanoDrop spectrophotometry. Subsequently, the DNA samples were amplified with the 515F-806R primers specific for the V4 hypervariable

regions of the 16S rDNA gene (5'-GTGCCAGCMGCCGCG GTAA-3' and 5'-ACTACHVGGGTWTCTAAT-3'). The PCR reactions were performed as described in our previous work [27]. Sequencing was performed on Illumina MiSeq platform according to the manufacturer's instructions, provided by Beijing Novogene Genomics Technology Co. Ltd. (China). Based on the unique barcode, the paired-end reads were assigned to samples and merged using FLASH. Subsequently, the raw tags were filtered under specific conditions to obtain high-quality clean tags according to the QIIME (V1.7.0). Sequences with  $\geq 97\%$  similarity were assigned to the same operational taxonomic units (OTUs) using the Uparse software package (Uparse v7.0.1001). The representative sequence for each OTU was screened, using the RDP classifier algorithm on the Green Gene Database to annotate taxonomic information.

To study the phylogenetic relationship between different OTUs, multiple sequence alignment was conducted using the MUSCLE software among the dominant species in different groups. The complexity of species diversity within one sample was compared by Alpha diversity analysis, including 6 factors i.e., ACE, Chao1, good-coverage, observed-species, Shannon, and Simpson; in contrast, the complexity of species diversity among different samples was compared by Beta diversity analysis.

### Cell proliferation assay for the metabolic products of *L. pentosus* and SCFAs

*L. pentosus* was grown in Soybean-Casein Digest Agar Medium (containing 15 g of casein trypsin digest, 5 g of soybean-papain digest, 5 g of sodium chloride, 15 g of agar in 1000 mL purified water, pH 7.3) at 37 °C for 24 h under microaerophilic conditions. After overnight culture, the medium contained *L. pentosus* at a concentration of  $4.5 \times 10^8$  CFU/mL. Then, it was diluted with fresh medium to  $2.0 \times 10^8$  CFU/mL and centrifuged at 1100 g for 15 min. The supernatant was filtered through a 0.2 mm membrane filter to remove the residual bacteria and debris. Subsequently, the pH of the supernatant was adjusted to 7.0 with 1 mol/L NaOH solution for the cell proliferation assay.

MTT [3-(4,5-Dimethylthiazol-2-yl)-2,5-diphenyltetrazolium bromide] staining assay was employed to investigate the effects of *L. pentosus* metabolites and SCFAs on CRC cell proliferation. Human CRC cell lines (HCT-116, HT-29, SW-480 for *L. pentosus* metabolites and HCT-116 for SCFAs) and normal colorectal epithelial (FHC) cells were cultured in DMEM supplemented with 15% FBS, 55 mg/mL streptomycin and 55 IU/mL penicillin at 37 °C in a humidified atmosphere with 5% CO<sub>2</sub>. Initially, cells from four different strains were transferred onto a 96-well culture plate at a density of 7000 cells/well. After overnight incubation, the cells were treated with 0.1% (final concentration, v/v) of

the supernatant above for different durations, or treated with different concentrations of SCFAs for 24 h. After further culture for 24 h at 37 °C, MTT reagent (20 µL, 1.5 mg/mL in PBS) was added to each well and the cells were further incubated for 4 h. Then, the supernatant was removed and 200 µL DMSO was added to each well to dissolve the intracellular formazan crystals. Finally, the relative survival rates of cells were obtained by measuring the absorbance of each well in a microplate reader at 490 nm.

### Hoechst staining

HCT-116 cells were seeded at a density of 7000 cells/well in a 96-well plate and were treated with 0.1% (v/v) of the *L. pentosus* metabolic product supernatant for 0, 8, 16, and 24 h. Subsequently, the cells were washed thrice with PBS, added with 5 µg/mL Hoechst 33,258, and then stained for 10 min at 37 °C in a humidified atmosphere containing 5% CO<sub>2</sub>. Morphological evaluations of nuclear condensation and fragmentation were carried out immediately after staining by a fluorescent microscope at 550 nm of emission.

### Flow cytometry

Apoptosis analysis was carried out by dual dye staining using Annexin V-EGFP/PI. HCT-116 cells ( $5 \times 10^4$  cells/well) were treated with the supernatant containing metabolic products of *L. pentosus* (0.05%, v/v) for 0, 8, and 16 h. Subsequently, cell apoptosis was detected using Annexin V and PI kit according to the manufacturer's instructions. The stained cells were subjected to a BD FACS Vantage SE Flow Cytometer (BD Biosciences, San Jose, CA, USA) and the results were analyzed using the Flow Jo 7.6.1 software (Tree Star Inc., Ashland, OR, USA).

### GC/MS analysis for SCFAs

The fecal samples (100 mg) were weighed and homogenized in 1.0 mL of methanol solution. After ultrasonic extraction for 10 min, sulfuric acid was used to adjust the pH of the suspensions to 3.0 and the samples were centrifuged at 3500 rpm for 10 min. The supernatants were filtered through a 0.2 mm membrane filter to remove the remaining fecal residue for the ensuing gas chromatography-mass spectrometry analysis using the Shimadzu GCMS-QP2010 mass spectrometer (EI mode, 70 eV) equipped with a Rtx-5MS capillary column (30 m × 0.25 mm × 0.25 µm). The gas flow rate was controlled at 1 mL/min with nitrogen as the carrier. The oven temperature was initially held at 100 °C for 0.5 min and raised to 180 °C at a rate of 8 °C per min. Then, it was raised to 200 °C at a rate of 20 °C per min and maintained at 200 °C for 5 min. The detector temperature was controlled at 240 °C and the inlet temperature was set

at 200 °C. The procedure time for each sample was 10.0 min and the injection volume of the samples was 1 µL.

### In vivo anti-tumor study of *L. pentosus* and SCFAs

Animal raising conditions were the same as mentioned in the Sect. 2.2. Twenty male BALB/c nude mice were randomly divided into four groups: *L. pentosus* (LAC), short chain fatty acids (SCFAs), NC, and TC groups. Each mouse in the LAC, SCFAs, and TC groups received inoculation with  $7 \times 10^6$  HCT-116 cells into the right foreleg. Mice were treated daily with *L. pentosus* ( $2 \times 10^8$  CFU/0.2 mL, suspended in purified water), or SCFAs (20 mM/0.2 mL, containing 71.5% of acetic acid, 11.8% of propionic acid, and 16.7% of butyric acid, according to the ratio of SCFAs in STGL-treated mice feces), or 0.9% saline solution by oral gavage. At day 30, mice were sacrificed; the organs and tumors were dissected to further explore the roles of *L. pentosus* and SCFAs in the development of CRC.

### Immunofluorescence study

Tumor tissues were dissected and fixed in 4% paraformaldehyde at 4 °C overnight followed by soaking in 10, 20 and 30% sucrose solutions for 24 h. Subsequently, they were cut into 30 µm sections and blocked in a solution containing 1% bovine serum albumin and 0.4% Triton X-100 for 2 h at room temperature. After that, tissue sections were incubated with rat anti-rabbit caspase-9 or caspase-3 primary antibody at 4 °C for 72 h. After washing with PBS, the sections were incubated with fluorescein isothiocyanate-conjugated anti-rabbit IgG secondary antibody in the dark for 2 h at room temperature. Finally, the sections were washed with PBS again, mounted on gel-coated slides and observed under a fluorescence microscope.

### Statistical analysis

Data were expressed as mean  $\pm$  SD. Statistical analysis was performed by the Duncan's Multiple Range Test using the SAS software package (Version 6.12, Cary, NC, USA). The *P*-value (probability) with *P* < 0.05 was considered as statistical difference and *P* < 0.01 was considered as significant difference.

## Results

### Inhibition of tumor growth by sitosterols

Following a test period of 30 days, the body weights of mice in the NC group reached  $24.88 \pm 2.49$  g, whilst those of the TC group decreased to  $18.72 \pm 2.45$  g. Sitosterol

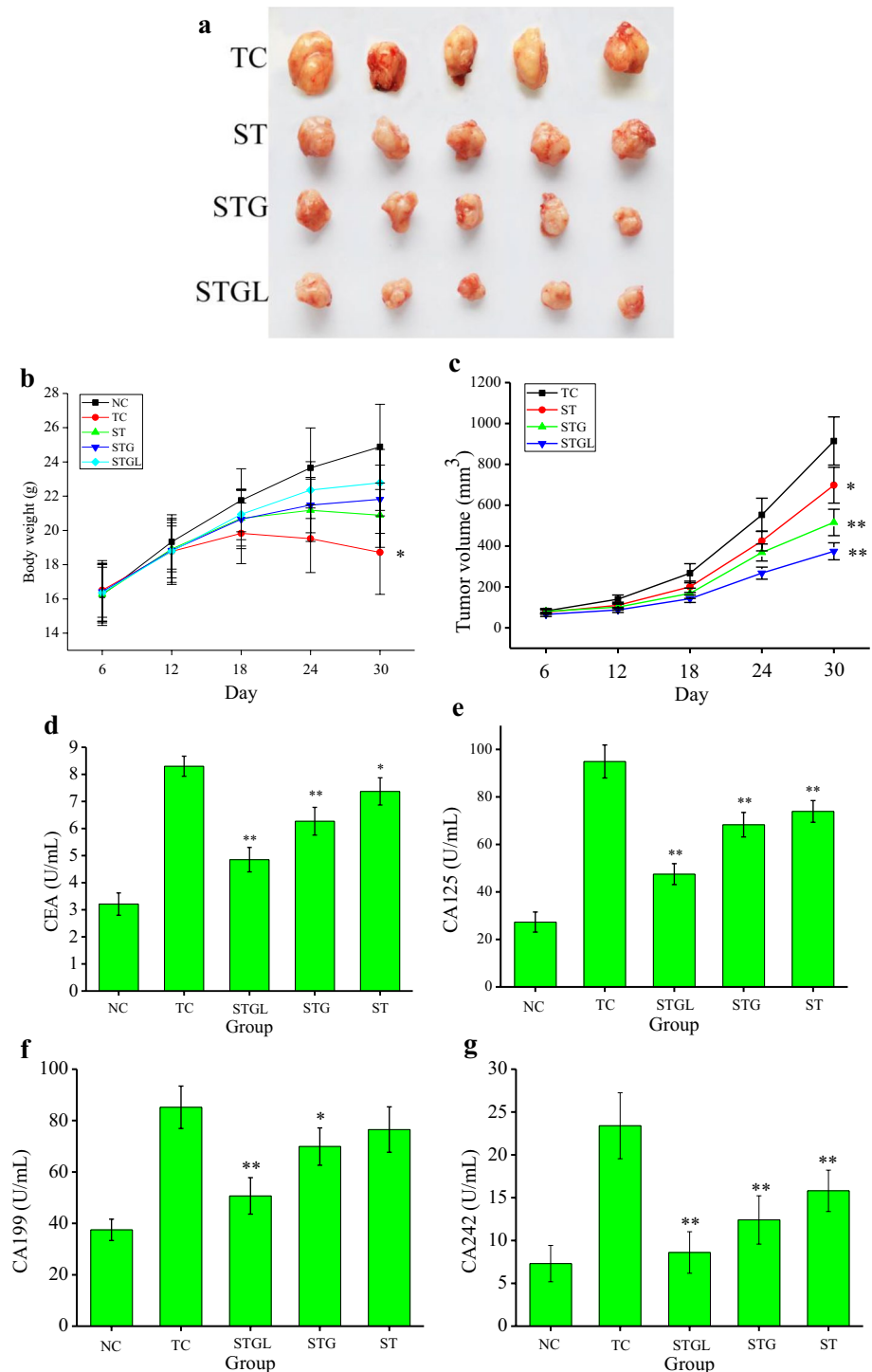
administration partly recovered the loss in body weight. Amongst the three drug groups, mice in the STGL group displayed higher average body weights of  $22.79 \pm 1.94$  g (Fig. 1b). Tumor volumes in the TC group were the highest, reaching  $914.2 \pm 117.7$  mm<sup>3</sup> at day 30 (Fig. 1a, c). STGL displayed the highest capacity to control tumor growth among the sitosterol-treated groups, achieving one-third of the average tumor volume of the TC group at day 30 ( $374.1 \pm 41.6$  mm<sup>3</sup>, *P* < 0.01). ST and STG also significantly suppressed tumor growth, with tumor volumes of  $697.8 \pm 87.9$  mm<sup>3</sup> and  $515.8 \pm 64.5$  mm<sup>3</sup> in ST and STG groups at day 30 (*P* < 0.05 and *P* < 0.01, compared with TC group), respectively.

Previous studies have shown that serum carbohydrate antigens and carcinoembryonic antigens including CEA, CA125, CA242 and CA199, are important biomarkers for clinical cancer diagnosis [28]. The serum levels of CA125, CA242 and CA199 in mice were measured using the multi-tumor marker protein chip diagnostic system. As shown in Fig. 1d–g, the levels of CEA, CA125, CA199 and CA242 in the TC group were significantly higher than those of the NC group. Following sitosterol treatment, the levels of the four tumor biomarkers declined, particularly following STGL treatment (CEA: 41.6% decrease, CA125: 49.9% decrease, CA199: 40.5% decrease, CA242: 63.2% decrease compared to the TC group, *P* < 0.01). These results indicate that sitosterols have beneficial anti-tumor effects.

### Tumor apoptosis

PI3K catalyzes the production of phosphatidylinositol-3,4,5-trisphosphate during cell survival and regulates cell metabolism and cytoskeletal rearrangements. As such, PI3K is pivotal to the growth and survival of cancer cells [29, 30]. We found that STG and STGL significantly (*P* < 0.01) inhibited PI3K/Akt in tumor tissue compared to untreated mice (Fig. 2a–c). The three sitosterols also altered the expression of apoptosis-related proteins (Bad, Bcl-cxl, cyto-c, caspase-9, caspase-3, and PARP) which are downstream effectors of PI3K/Akt signaling (Fig. 2d–j). Bad expression increased up to 61.9% and 42.8% in the STGL and STG groups, compared to the TC group, respectively (*P* < 0.01). Bcl-xl levels decreased by 56.9% and 34.3% in the STGL and STG groups (*P* < 0.01). Moreover, the production of cyto-C was enhanced by STGL and STG treatment. The expression of cleaved-caspase-9 increased 73.9% and 60.9% in the STGL and STG groups respectively (*P* < 0.01). The expression of cleaved-caspase-3 increased by 81.5% and 52.3% in STGL and STG-treated groups, respectively (*P* < 0.01). Accordingly, the total levels of uncleaved PARP (116 kD) significantly decreased in the sitosterol-treated groups, whilst the levels of cleaved PARP (89 kD) increased (*P* < 0.01).

**Fig. 1** Sitosterols suppressed tumor growth in mice. Mice in the TC, ST, STG, STGL groups were injected with HCT-116 tumor cells. The tumor-bearing mice were treated daily with 60 mg/kg of sitosterols or 0.2 mL of 0.9% saline solution by intragastric gavage for 30 days ( $n=5$  in each group). After sacrificing, tumor tissues were stripped and serum carcinoembryonic antigen CEA and carbohydrate antigens CA125, CA242 and CA199 were measured. **a** The appearance of tumors in each group. **b** Body weight gain. **c** Tumor volume gain. **d** Level of CEA. **e** Level of CA125. **f** Level of CA199. **g** Level of CA242. Data were expressed as mean  $\pm$  SD. Statistical comparisons were performed by one-way ANOVA analysis and two-sample student's *t* tests. \* $P < 0.05$ , \*\* $P < 0.01$  versus TC group



Immunohistochemistry was performed on tumor tissue to assess caspase-9 and caspase-3 distribution as an indicator of tissue proliferation and apoptosis. As shown in Fig. 2k–n, sitosterol treatment significantly increased caspase-9 and caspase-3 expression, the most notable increase occurring in STGL treated groups. The levels of apoptosis as assessed by TUNEL staining were also higher in the sitosterol-treated groups (Fig. 2o). Taken together, these data reveal that

sitosterol administration induces tumor apoptosis through PI3K/Akt signaling and caspase-3 activation in mice.

### Alteration of gut microbiota structure

To determine if the anti-CRC effects of sitosterols in mice are associated with changes of gut microbiota, 16S rDNA Illumina sequencing was performed in fecal samples.

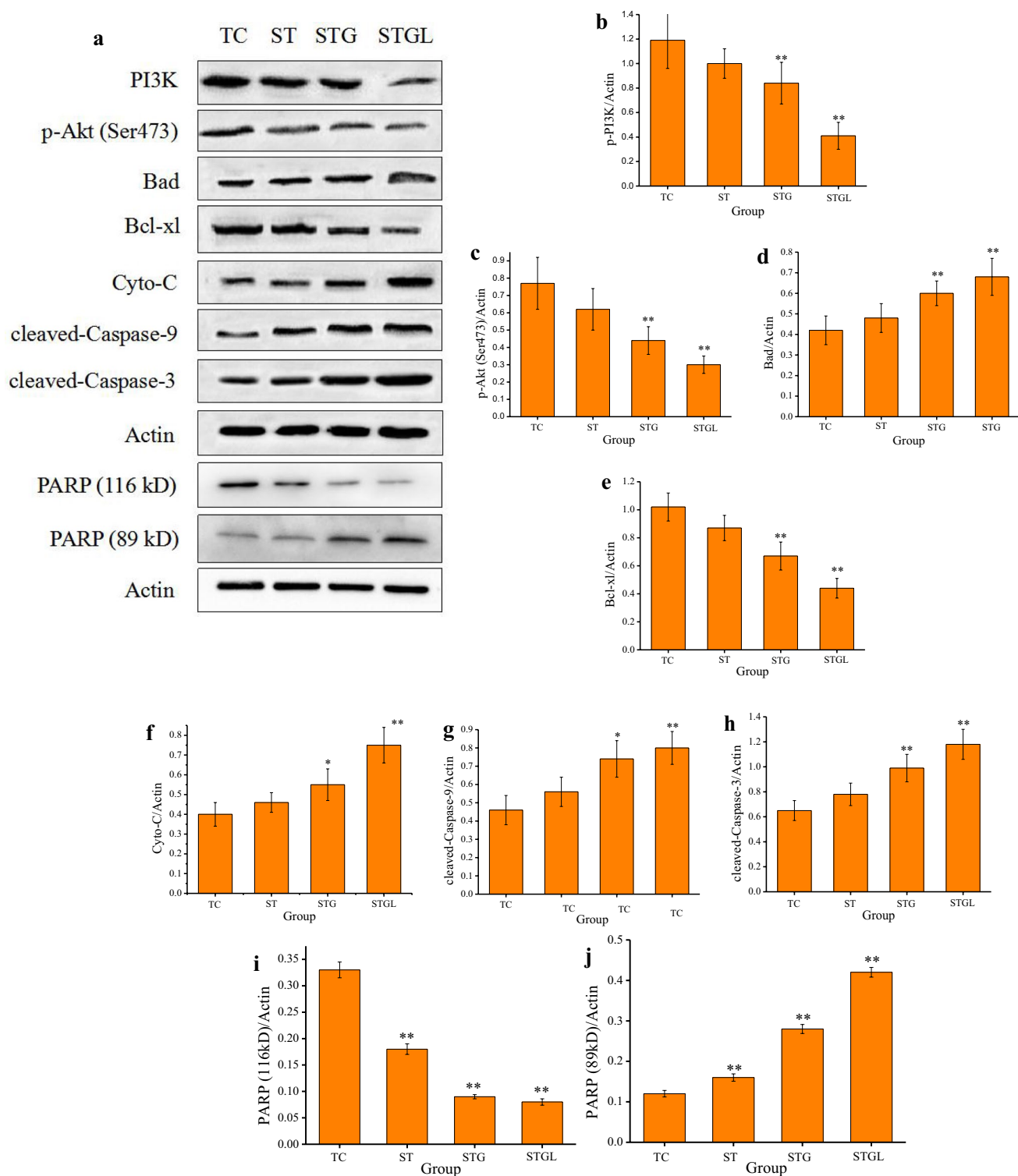


**Fig. 2** Expression of PI3K/Akt and the downstream signaling transduction pathway in tumor tissues by western blotting, as well as the immunohistochemical analysis of caspase-9 and caspase-3. Tumor tissues from mice which were treated with 60 mg/kg/d of ST, or STG, or STGL were used for western blotting (n=5 per group). **a–j** The expressions of p-PI3K, p-Akt (Ser473), Bad, Bcl-xl, cyto-C, cleaved-caspase-9, cleaved-caspase-3, and PARP. **k–l** Three representative panels of caspase-9 or caspase-3 staining of the tumor tissues in each

group (10 sections for each group); image magnification:  $\times 20$ . **m** Mean caspase-9 score in each group. **n** Mean caspase-3 score in each group. **o** TUNEL checking for tumor tissues (n=5); image magnification:  $\times 20$ . Data were expressed as mean  $\pm$  SD. Statistical comparisons were performed by one-way ANOVA analysis and two-sample student's *t* tests. \* $P < 0.05$ , \*\* $P < 0.01$ , # $P < 0.05$ , ## $P < 0.01$ , compared with the TC group

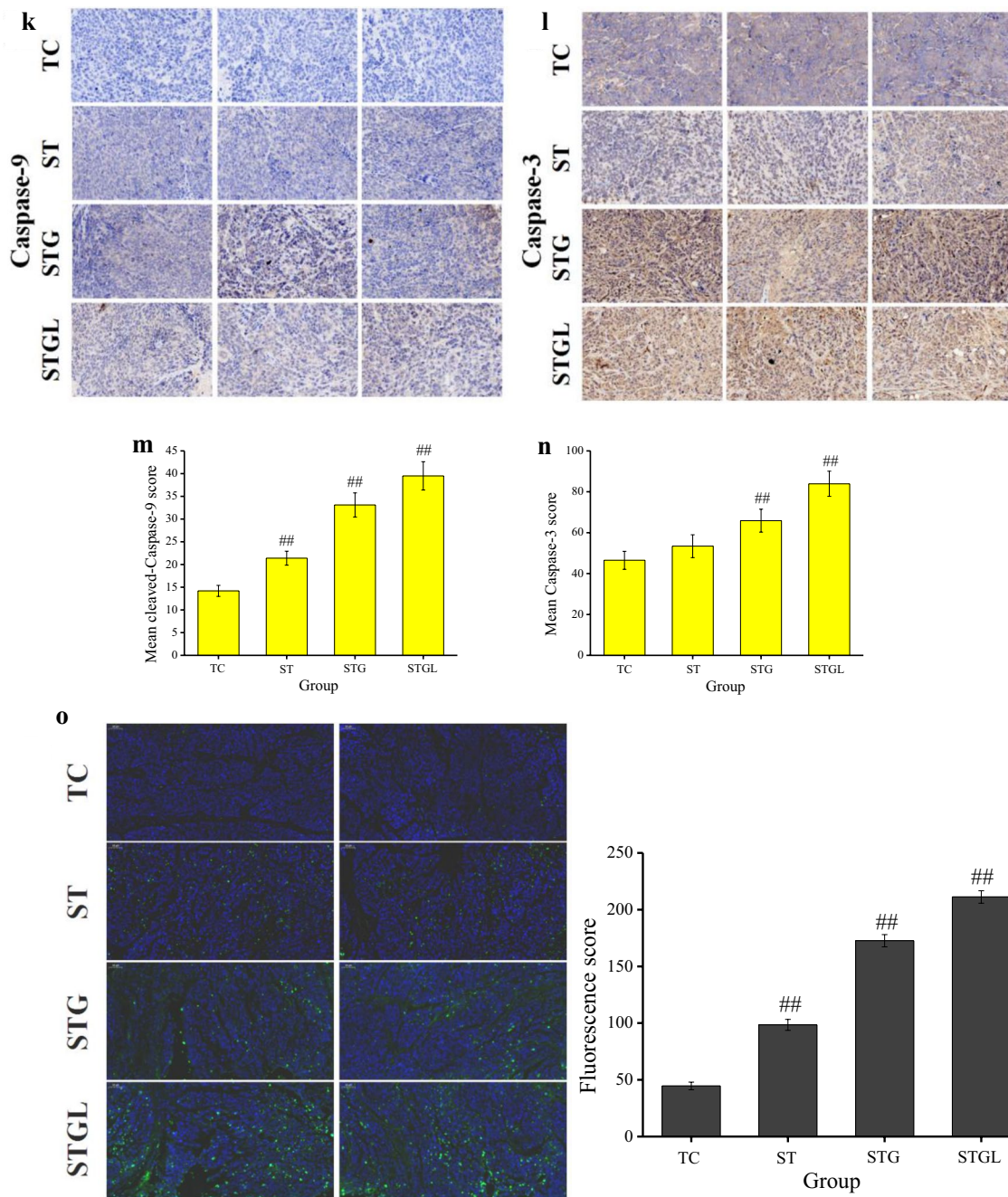
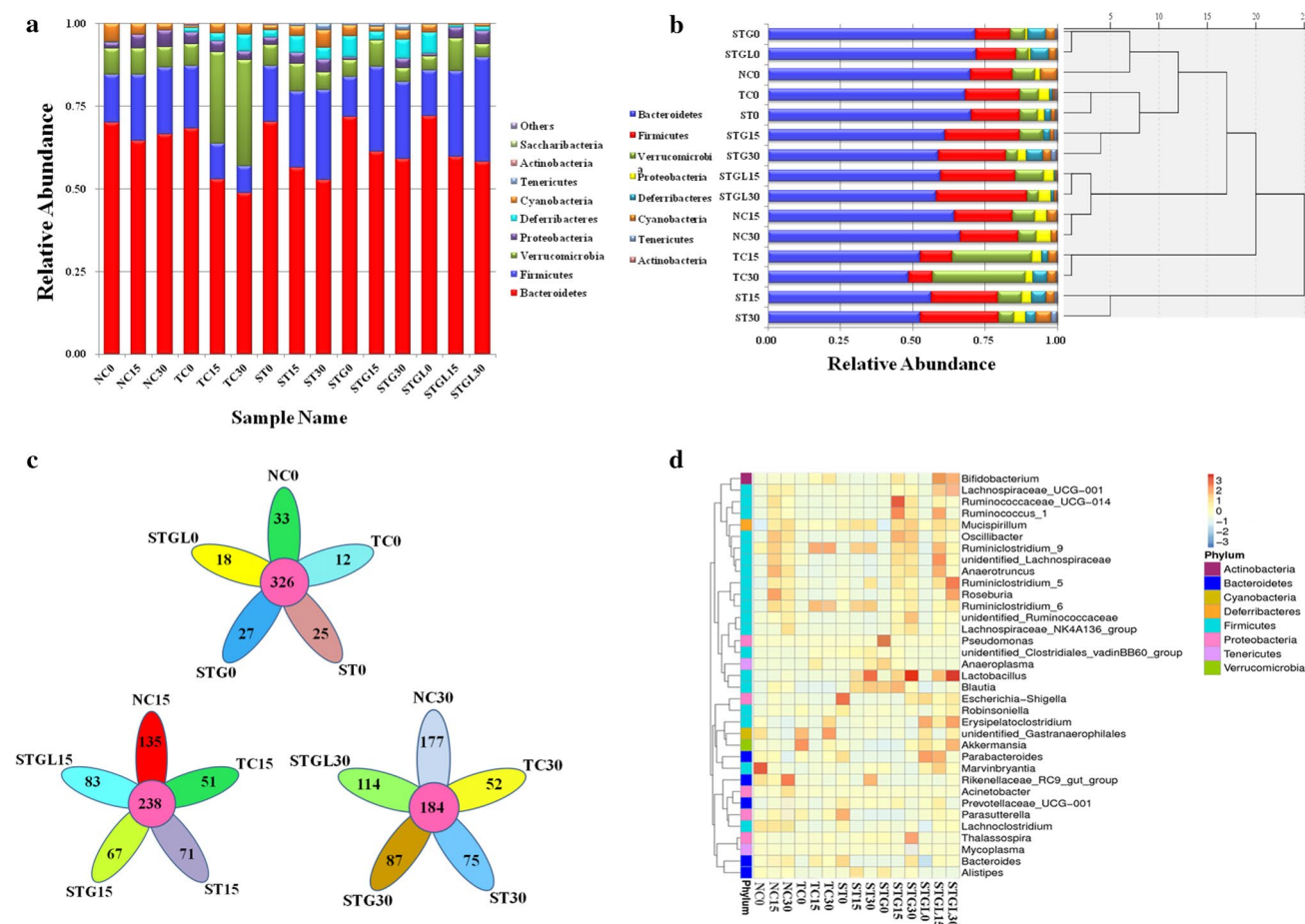


Fig. 2 (continued)

Using 97% identity clustering analysis, sequences were classified into 815 OTUs. Taxonomic profiling demonstrated non-significant microbiota variations in the NC group over the experiment period (Fig. 3a). The proportions of phyla *Bacteroidetes* and *Firmicutes* decreased in the TC group over time, whilst *Verrucomicrobia* increased. Interestingly, sitosterol treatment reinforced the proportion of *Firmicutes* and reduced the relative abundance of *Verrucomicrobia*. A general survey of the microbiological

composition through the feeding period revealed little difference between days 15 and 30 in each group, indicating the formation of a relatively stable microbial community after 15 days. UPGMA clustering of the top 10 phyla of gut microbiota based on Weighted Unifrac distance indicated a statistically significant separation between NC, TC and sitosterol treated groups (Fig. 3b). Differences were also observed between the ST-treated group and STG- or





**Fig. 3** Sitosterols altered the gut microbiota composition in mice. Microbiota composition at day 0, 15, and 30 in faeces of mice in the NC group or in the sitosterols-treated group ( $n=5$  for each group). **a** Taxonomy classification of top 10 reads at the phylum level over time. **b** Unweighted pair-group method with arithmetic mean (UPGMA) clustering analysis of top 10 intestinal bacteria at the phylum level based on Weighted Unifrac distance. **c** Operational taxo-

mic unit (OTU) analysis of the gut bacterial community in different groups at the same time points. Each petal represents one group and the number on it denotes its particular OTUs. The numbers in the center represent the communal OTUs to all groups. Sequences beyond 97% identity were clustered into one OTU. OTUs are organized according to their phylogenetic positions. **d** Heat map formed by the redundancy analysis of top 35 genera of each group

STGL-treated groups, which may be associated with the superior ability of STG and STGL to inhibit tumor growth.

The total number of bacterial phylotypes in each group were classified into OTUs and shown as petals in Fig. 3c. The number on a petal denotes the particular OTUs for one group, otherwise, it represents the communal OTUs to all groups when located centrally. The total gut microbiota diversity increased with time: only 441 OTUs were evident on day 0, which increased to 645 at day 15, reaching 689 at day 30. The numbers in the center of petals i.e. the OTUs existing in all groups declined over time, from 326 at day 0, to 238 at day 15, which decreased to 184 at day 30. As for each individual group, gut microbiota diversity in the NC group maintained a relatively steady abundance of approximately 360 OTUs throughout the experiment period. However, a decreased of 338–236 occurred in the TC group. This illustrated that tumor growth reduced the diversity of gut

microbiota. Sitosterol treatment led to the improvement of bacterial species in mice and 298 OTUs were observed in the STGL-treated group at day 30.

Redundancy analysis (RDA) was employed to identify the specific bacterial phylotypes at the genus level that were altered during tumor-growth and sitosterol treatment. As shown in Fig. 3d, amongst the top 35 genera, the proportions of more than 10 genera in phylum *Firmicutes* reduced in tumor-bearing mice. Interestingly, treatment with sitosterols prevented this decline and improved the diversity of microbiota. The relative bacterial abundance in STG- and STGL-treated groups were richer than those of the TC group. Notably, *Lactobacillus* was present in low proportions in NC and TC groups, whilst sitosterol treatment led to an enrichment of *Lactobacillus* to different extents in the treated groups. These results indicated that sitosterols are beneficial to the recovery of the diversity of gut microbiota

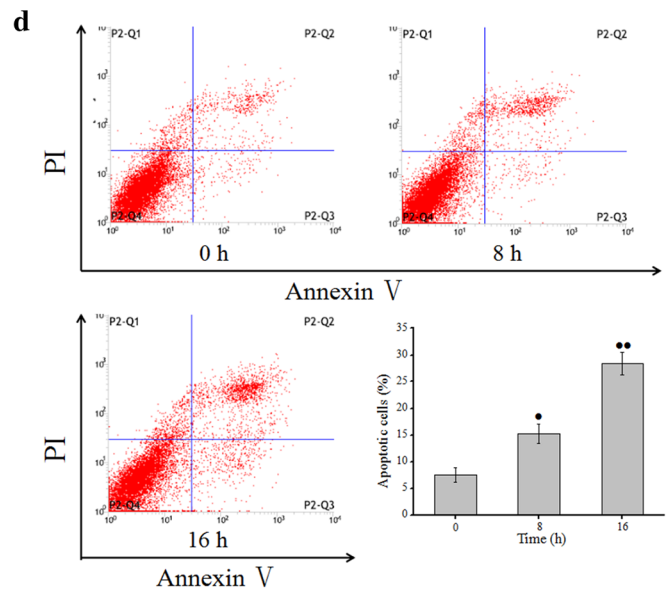
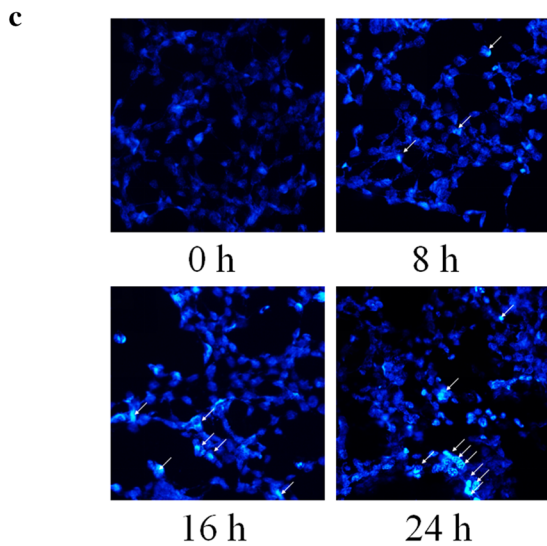
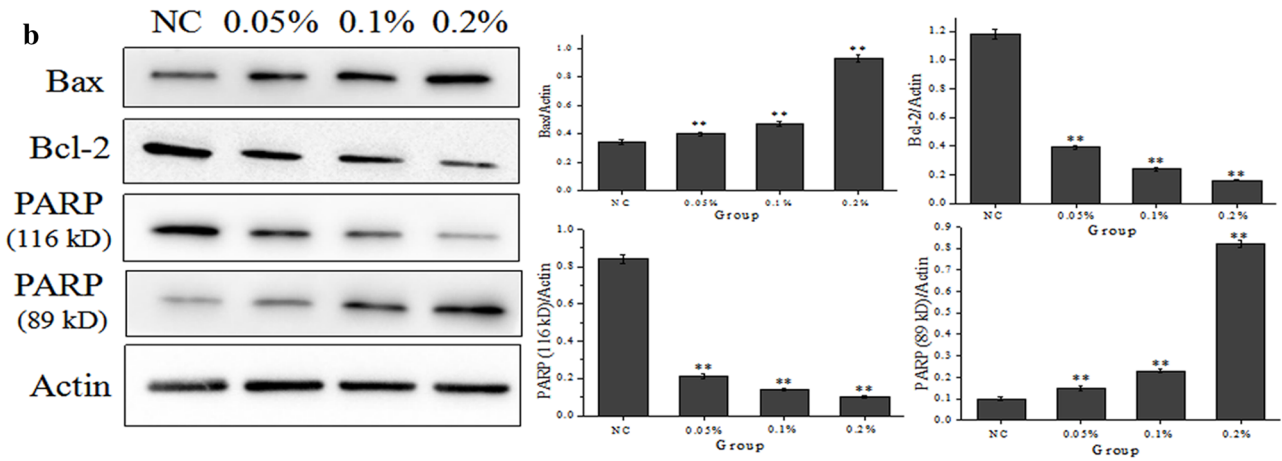
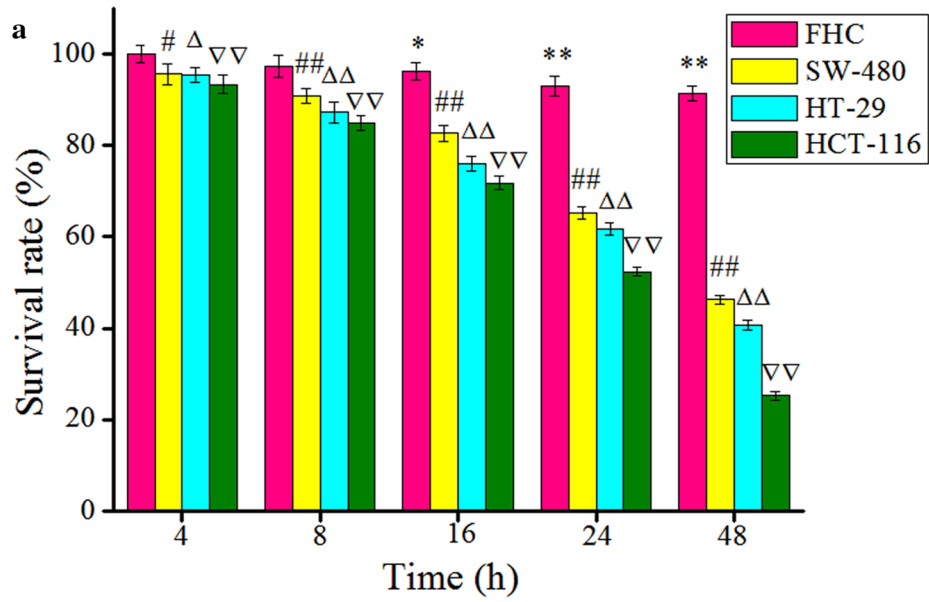


**Fig. 4** *L. pentosus*'s metabolic products induced apoptosis in vitro. After culturing over night, the Soybean-casein digest agar medium containing *L. pentosus* at  $4.5 \times 10^8$  CFU/mL. The medium was diluted to contain *L. pentosus* at  $2.0 \times 10^8$  CFU/mL and filtered by a 0.2 mm membrane to remove the bacteria and debris; the supernatant was used as the metabolites. **a** The inhibitory effect of 0.1% of the supernatant on the proliferation of FHC, SW-480, HT-29, and HCT-116 cells at different treated times (n=6). \* $P < 0.05$ , \*\* $P < 0.01$ , # $P < 0.05$ , ## $P < 0.01$ ,  $\Delta P < 0.05$ ,  $\Delta\Delta P < 0.01$ ,  $\nabla P < 0.05$ ,  $\nabla\nabla P < 0.01$ , versus the untreated group of each cell line. **b** Western blot results for HCT-116 cells after the cells were treated with 0.05%, 0.1%, or 0.2% of the metabolites for 24 h. \*\* $P < 0.01$  **c** Hoechst staining for HCT-116 cells after treatment with 0.1% of the metabolites for 0, 8, 16, and 24 h. **d** Annexin V-EGFP/PI staining of HCT-116 cells after treatment with 0.05% of the supernatant for different time periods. Representative scatter plots of PI (y-axis) versus annexin V (x-axis) (n=6). \* $P < 0.01$ , \*\* $P < 0.01$ , compared with 0 h. Data were expressed as mean  $\pm$  SD. Statistical comparisons were performed by one-way ANOVA analysis and two-sample student's *t* tests

that was reduced by tumor-growth, maintaining an abundant bacterial community in mice.

The top 10 most altered bacteria species whose relative content in the NC group exceeded 0.1‰ were counted and are presented in Table S1. The most amplified species in the TC group was *Lachnospiraceae\_bacterium\_A2* (19.036 fold increase compared to the NC group) whilst *Robinsoniella\_sp.\_KNHs210* decreased to the greatest levels (83.8% decline compared to the NC group). However, *L.\_bacterium\_A2* was almost eliminated in the gut of STG- and STGL-treated mice. As for ST treated mice, the largest increase in bacterial species was *L.\_bacterium\_COE1* that had a relative abundance 27.741 fold higher than the NC group, followed by *L. pentosus* which was 26.136 fold higher. In addition, *L. pentosus* had the largest increase in both STG and STGL groups, reaching 108.773 and 166.045 fold augmentation, respectively.

### ***L. pentosus*'s metabolic products induce apoptosis in vitro**

Due to the abundance of gut *L. pentosus* in sitosterol-treated mice, we explored the effects of this bacteria on CRC. Supernatants of Soybean-Casein Digest Agar Medium in which *L. pentosus* was cultured overnight and thus contained bacterial metabolites, was assessed in CRC cell proliferation assays. As shown in Fig. 4a, the metabolites displayed no obvious toxicity to normal colorectal epithelial FHC cells (viability  $\geq 90\%$ ). The proliferation of HCT-116 cells was, however, significantly inhibited ( $P < 0.01$ ) in a time-dependent manner, reaching 47.6% and 73.7% inhibition at 24 h and 48 h, respectively. Similarly, the metabolites inhibited the proliferation of SW-580 and HT-29 cells 34.7% and 39.2% after 24 h, which decreased to 53.7% and 59.4% after 48 h, respectively. Western blot analysis showed that PARP levels decreased in response to the metabolites, whilst

Bax expression decreased and Bcl-2 expression increased (Fig. 4b). The levels of cleaved-PARP increased 1.3- and 7.2-fold in the presence of 0.1% and 0.2% of the metabolites. In the 0.2% metabolite-treated group, Bax expression increased by 173.5%, whilst Bcl-2 expression decreased by 86.4%.

The number of apoptotic cells with condensed or fragmented chromatin also increased in a time-dependent manner (Fig. 4c). The effect of the *L. pentosus*'s metabolites on the apoptosis of HCT-116 cells was assessed by Annexin V-EGFP/PI staining and flow cytometry. As shown in Fig. 4d, the number of apoptotic cells increased to  $15.3 \pm 2.5\%$  at 8 h and  $28.4 \pm 2.3\%$  at 16 h, in comparison with  $7.5 \pm 1.8\%$  in the NC group. Both Hoechst and annexin V-EGFP/PI staining confirmed the ability of the *L. pentosus*'s metabolites to induce apoptosis in vitro.

### **SCFAs levels increase in sitosterol-treated mice**

Since we detected microbiota shifts in the fecal samples and their potential role in CRC cell apoptosis, we next assessed the nature of the metabolites that mediate these effects. We analyzed the SCFA content of fresh faecal samples of sitosterol-treated and untreated mice by gas chromatography-mass spectrometry (Fig. S2). There were no significant differences in the content of propionic acid and butanoic acid between the fecal samples of TC and ST groups, but the levels of acetic acid significantly increased in the ST group ( $18.27 \pm 2.81\%$  vs.  $3.50 \pm 0.58\%$ ,  $P < 0.01$ ). In STG-treated mice, both acetic acid and propionic acid were considerably higher than the TC group ( $P < 0.01$ ). In particular, the relative content of acetic acid in the STGL-treated group increased to  $32.13 \pm 2.10\%$  ( $P < 0.01$ ), whilst the propionic acid content reached  $5.32 \pm 0.61\%$  (from  $0.45 \pm 0.18\%$  in the TC group,  $P < 0.01$ ). The butanoic acid content reached  $7.51 \pm 0.78\%$  (from  $0.25 \pm 0.07\%$  in the TC group,  $P < 0.01$ ).

### **SCFAs promote apoptosis in vitro**

The inhibitory effects of SCFAs on HCT-116 cells were confirmed in cell proliferation assays. After treatment for 24 h, a concentration-dependent decrease in cell proliferation occurred in response to SCFAs. When treated with acetic acid at concentrations of 0.125  $\mu\text{L/mL}$  and 2.0  $\mu\text{L/mL}$  (v/v), the relative survival rates of the cells were  $92.33 \pm 0.74\%$  and  $17.07 \pm 1.38\%$ ; compared to  $91.26 \pm 0.81\%$  and  $27.93 \pm 1.65\%$  in the propionic acid group, and  $56.64 \pm 1.46\%$  and  $25.19 \pm 1.81\%$  in the butanoic acid group ( $P < 0.01$ ) (Fig. 5a).

Western blot assays were used to assess the expression of apoptotic proteins in HCT-116 cells cultured in 0.5  $\mu\text{L/mL}$  acetic acid, propionic acid, or butanoic acid for 24 h. All three treatments suppressed PI3K/Akt activation and

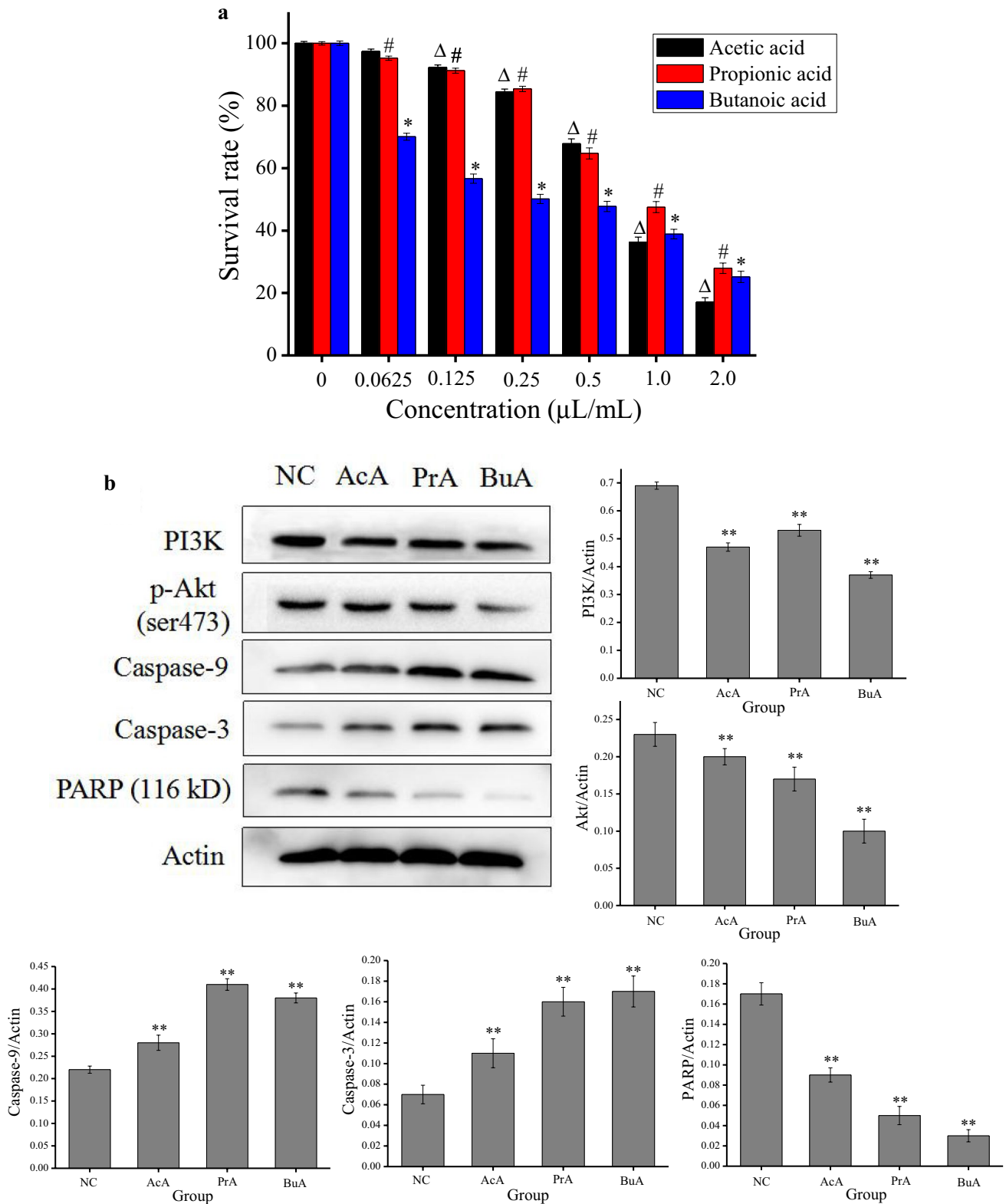


**Fig. 5** SCFAs promoted cell apoptosis in vitro. **a** The inhibitory effect of SCFAs on the proliferation of HCT-116 cells at different concentrations for 24 h (n=6). \* $P < 0.01$ , # $P < 0.01$ ,  $\Delta P < 0.01$ , versus the untreated group. **b** Western blot results after treating HCT-

116 cells with 0.5  $\mu\text{L/mL}$  of SCFAs for 24 h. *NC* normal control group, *AcA* acetic acid group, *PrA* propionic acid group; *BuA* butanoic acid group. \*\* $P < 0.01$ , versus TC group. Data were expressed as mean  $\pm$  SD

the expression of caspase-9 and caspase-3. PI3K levels decreased 31.9% in the acetic acid group, 23.2% in the propionic acid group, and 46.4% in the butanoic acid group, all of which were significant ( $P < 0.01$ ). Caspase-3 expression increased by 57.1% in the acetic acid group, 128.6% in the propionic acid group, and 142.8% in the butanoic acid group ( $P < 0.01$ ). The levels of uncleaved PARP significantly decreased in SCFAs treated cells. Acetic acid decreased PARP expression by 47.0%, compared to 70.6% in the propionic acid group, and 82.4% in the butanoic acid group (Fig. 5b).

### ***L. pentosus* and SCFA decrease tumor development in vivo**

Due to the change in content of the SCFAs in the faeces of the mice, we speculated their negative association with tumor growth. SCFAs from *L. pentosus* culture medium were analyzed in which 3.89% acetic acid, 1.76% propionic acid, and 2.84% butyric acid were present (Fig. S3a, b). No SCFAs were present in the initial composition, highlighting that *L. pentosus* is capable of producing SCFAs. We investigated HCT-116 cells growing as xenograft tumors in BALB/c nude mice to explore the anti-cancer effects of *L. pentosus* and SCFAs. Mice were treated daily with *L. pentosus* ( $2 \times 10^8$  CFU/0.2 mL), SCFAs (20 mM/0.2 mL, containing 71.5% acetic acid, 11.8% propionic acid, and 16.7% butyric acid, according to the ratio of SCFAs in the STGL-treated mice faeces), or 0.9% saline solution for 30 days. The results showed that SCFAs and *L. pentosus* similarly improved tumor-induced weight loss (Fig. S3d). Distinct inhibitory effects on tumor growth were observed in both LAC and SCFAs groups over the treatment period (Fig. S3c, e). *L. pentosus*-treated mice had the slowest tumor growth rates compared to those receiving no therapy or SCFAs (61.5% of the tumor volume of mice in the TC group,  $585.9 \pm 41.7$  mm<sup>3</sup> versus  $952.3 \pm 54.6$  mm<sup>3</sup>).

In addition, *L. pentosus* and SCFAs reduced PI3K-Akt-related expression resulting in caspase-3 activation and tumor apoptosis. As shown in Fig. 6a–h, a significant decrease in p-PI3K was observed in mice administered *L. pentosus* and SCFAs for 30 days (30.5% and 67.4% decrease, respectively), ( $P < 0.05$ ). The expression of the downstream signaling proteins p-Akt (Ser473), Bad, Bcl-x1, cyto-C, cleaved-caspase-9, and cleaved-caspase-3 showed a similar trend. SCFA-treated mice also displayed elevated levels of bad expression, but this increase was not significant in comparison to the TC group. Caspase-3 increased by 32.1% and 101.5% after treatment with SCFAs and *L. pentosus*, respectively. Caspase-9 and caspase-3 were redistributed and highly expressed in CRC tumors treated with *L. pentosus*- and SCFA, confirming their ability to induce apoptosis (Fig. 6i–l).

## **Discussion**

CRC is the third most common form of cancer and the second leading cause of cancer-related deaths in the western world [31]. ST and STG, but not STGL, exist in natural plants and were extracted from sweet potato in this study. The three compounds showed no anti-tumor effects in vitro on HCT-116, HT-29 or SW-480 cells even at their saturated solubility in water ( $< 0.1$  mg/mL). When these compounds were administered to tumor-bearing mice, the growth of tumors was significantly arrested.

In 1996, the American Society of Clinical Oncology (ASCO) first published evidence-based clinical practice guidelines for the use of tumor markers in breast cancer [32]. In addition, with the advances in genomic technologies, multiparameter detection of serum carbohydrate antigens and carcinoembryonic antigens have been practiced clinically. Our results indicate that the serum tumor biomarkers CEA, CA125, CA242 and CA199 significantly increased in the TC group, but decreased following sitosterol treatment, particularly in the STGL group. Genes in the PI3K/AKT signaling axis are the most frequently mutated networks in human cancer; moreover, aberrant activation of this pathway is related to tumorigenesis, cancer progression, and drug resistance [33]. Diverse targets in this pathway include AKT, p110, p85, mTOR, and PTEN, providing multiple areas of anti-cancer therapeutic intervention [34–37]. We found that STG and STGL administration remarkably reduced the phosphorylation of PI3K and Akt (Ser473) in tumor tissue. Decreased PI3K/Akt activity resulted in enhanced Bad expression in sitosterol-treated mice. Furthermore, Bcl-x1, a mitochondrial protein that is regulated by Bad, displayed reduced expression. The release of cyto-C from the mitochondrial intermembrane space into the cytosol is an important phenomenon in caspase-dependent tumor apoptosis [38]. We observed that the release of cyto-C increased in sitosterol-treated mice when Bcl-x1 expression decreased. Accordingly, caspase-9 and caspase-3 levels increased in sitosterol-treated mice, enhancing PARP cleavage. This led to sitosterol induced apoptosis, observed by immunohistochemistry and TUNEL staining.

The diverse community of bacteria in the human gut plays regulate host metabolism and immunity, in addition to the digestion and conversion of dietary constituents [39, 40]. Approximately 20% of human malignancies are associated with bacteria and the relationship between cancer and microbes is complex [41]. Harmful microbes lodged in mucosal sites can become part of the tumor microenvironment of aerodigestive tract malignancies. In addition, intratumoral bacteria can affect the growth and metastasis of tumors [42–45]. In contrast, salutary microorganisms

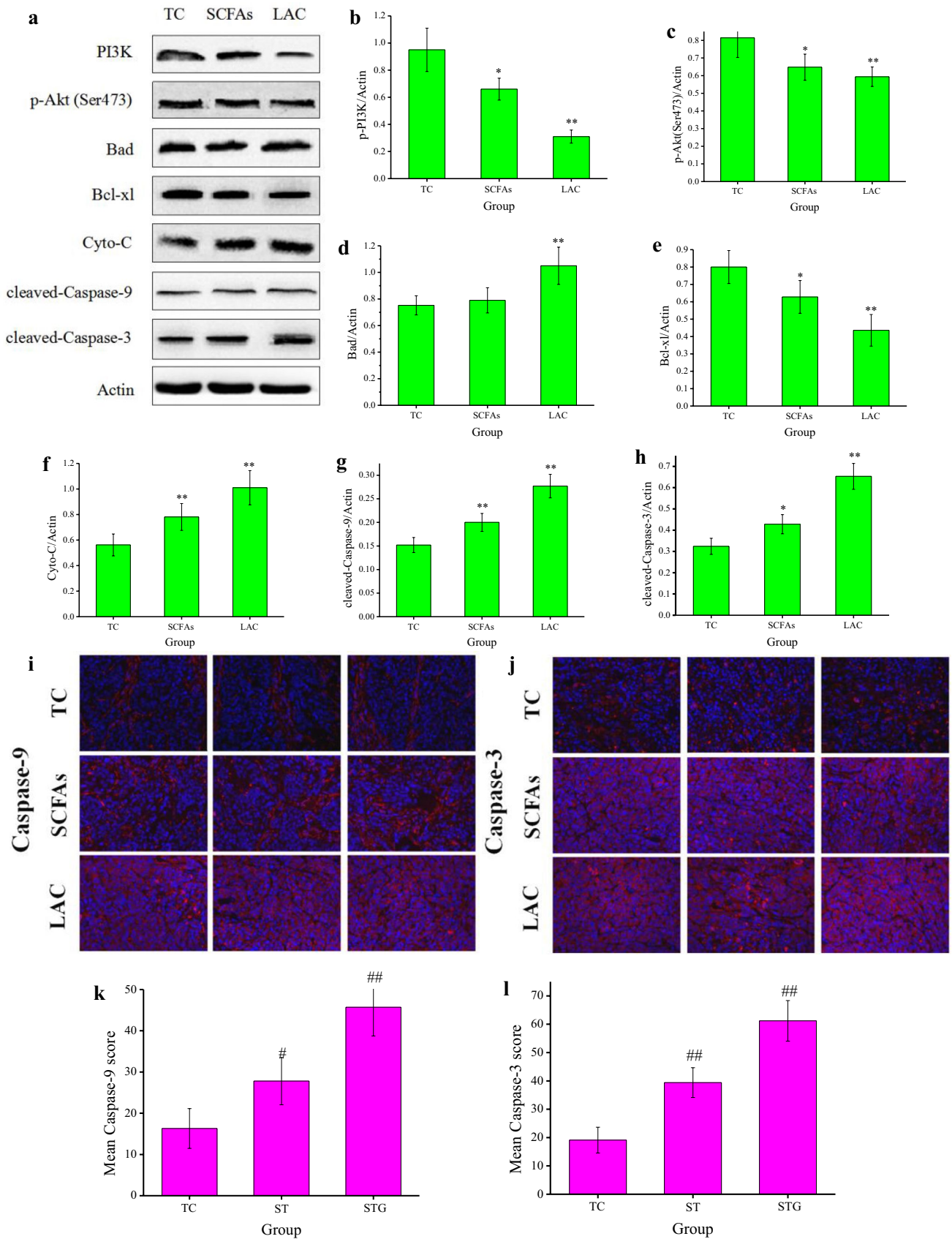


**Fig. 6** Re-detection of PI3K/Akt signaling pathways after the mice were treated with *L. pentosus* and SCFAs, along with the immunofluorescence staining of caspase-9 and caspase-3. Tumor tissues were obtained from mice which were treated with  $2 \times 10^8$  CFU/0.2 mL of *L. pentosus*, 20 mM/0.2 mL of SCFAs, or 0.2 mL of 0.9% saline solution ( $n=5$  per group). **a–h** The expression of p-PI3K, p-Akt (Ser473), Bad, Bcl-x1, cyto-c, cleaved-caspase-9, and cleaved-caspase-3. **i–j** Three representative sections of immunofluorescence staining for caspase-9 and caspase-3 expressed in tumor tissues (10 panels for each group). Image magnification:  $\times 400$ . **k** Mean caspase-9 score in each group. **l** Mean caspase-3 score in each group. \* $P < 0.05$ , \*\* $P < 0.01$ , # $P < 0.05$ , ## $P < 0.01$ , versus TC group. Data were expressed as mean  $\pm$  SD. Statistical comparisons were performed by one-way ANOVA analysis and two-sample student's *t* tests

in the gut are involved in detoxifying dietary components, reducing inflammation, and maintaining a balance during host cell growth and proliferation [46]. Our analysis of the gut microbiota of mice revealed that tumor growth dramatically reduced the diversity of gut microbiota, particularly in the phyla *Bacteroidetes* and *Firmicutes*. Interestingly, treatment with sitosterols reversed this decrease. The genus *Lactobacillus* were in small proportions in both normal and tumor-bearing mice, but sitosterols largely enriched its abundance in the gut. *L. pentosus*, which is beneficial to the human body and shows strong resistance to the acidic environment of the gastrointestinal tract [46, 47] increased 166.045 fold in STGL-treated mice. The metabolites of *L. pentosus* inhibited the growth of HCT-116, HT-29, and SW-480 CRC cells and induced their apoptosis. In confirmatory experiments in tumor-bearing mice, *L. pentosus* at a daily dose of  $2 \times 10^8$  CFU/0.2 mL inhibited tumor growth through the induction of apoptosis. The relationship between *L. pentosus* and CRC is rarely reported. We have illustrated that gut microbiota play a vital role in cancer development and sitosterols are beneficial for maintaining a healthy and diverse bacterial community.

SCFAs are the major fermentative products of carbohydrates and proteins of bacteria in the gut [48, 49]. SCFAs mediate many of the functions assigned to the microbiota through classical endocrine signaling such as modulating the release of enteroendocrine serotonin (5-HT) and peptide YY (PYY) [50, 51]. As the gut microbiota diversity of mice improves in response to sitosterols, the concentration of SCFAs in the gut simultaneously increase. The ability of acetic acid, propionic acid, and butanoic acid to induce tumor cell apoptosis was confirmed both in vitro and in vivo. Remarkable tumor apoptosis induction was observed following daily treatment with 20 mM/0.2 mL SCFAs. Reduced tumor growth in response to acetate occurred as a consequence of the suppression of ACSS2 and lipid synthesis [27, 52]. Thus, SCFAs display anti-cancer properties through inducing tumor cell apoptosis.

In summary, we have demonstrated that sitosterols can maintain a diverse gut microbial milieu and enrich the abundance of beneficial bacteria such as *L. pentosus*. This leads to the production of valuable metabolites, especially the SCFAs, which weaken the signal transduction of PI3K/Akt and change the expression levels of several apoptosis-related proteins, ultimately resulting in tumor apoptosis. Thus, our work may provide a novel strategy for using dietary supplements to enhance the gut microbiota to ameliorate cancers, especially the digestive tract cancers.

**Acknowledgements** This work was financially supported by the Special Program for Scientific and Technical Innovation of Chongqing Social Livelihood (cstc2015shmszx80012, cstc2017shms-kjfp80004), Fundamental Research Funds for the Central Universities (XDJK2017D151, XDJK2017D160), Chongqing Postgraduate Research and Research Innovation Project (CYS17068), Achievement Transfer Program of Institutions of Higher Education in Chongqing (KJZH17105), and County-University Cooperation Innovation Funds of Southwest University (Zx201601).

## Compliance with ethical standards

**Conflict of interest** The authors declare that there are no potential conflicts of interest.

## References

1. Arnold M, Sierra MS, Laversanne M, Soerjomataram I, Jemal A, Bray F (2017) Global patterns and trends in colorectal cancer incidence and mortality. *Gut* 66(4):683–691
2. Siegel RL, Miller KD, Jemal A (2018) Cancer statistics, 2018. *CA Cancer J Clin* 68(1):7–30
3. Akin H, Tözün N (2014) Diet, microbiota, and colorectal cancer. *J Clin Gastroenterol* 48:S67–S69
4. Sears CL, Garrett WS (2014) Microbes, microbiota, and colon cancer. *Cell Host Microbe* 15(3):317–328
5. Hagggar FA, Boushey RP (2009) Colorectal cancer epidemiology: incidence, mortality, survival, and risk factors. *Clin Colon Rectal Surg* 22(4):191–197
6. Siegel RL, Miller KD, Jemal A (2015) Cancer statistics, 2015. *CA Cancer J Clin* 65(1):5–29
7. Yang D, Zhang M, Gold B (2017) Origin of somatic mutations in beta-catenin versus adenomatous polyposis coli in colon cancer: random mutagenesis in animal models versus nonrandom mutagenesis in humans. *Chem Res Toxicol* 30(7):1369–1375
8. Vano YA, Rodrigues MJ, Schneider SM (2009) Epidemiological link between eating habits and cancer: the example of colorectal cancer. *Bull Cancer* 96(6):647–658
9. Vargas AJ, Thompson PA (2012) Diet and nutrient factors in colorectal cancer risk. *Nutr Clin Pract* 27(5):613–623
10. Sinha R, Chow WH, Kulldorff M, Denobile J, Butler J, Garcia-Closas M, Weil R, Hoover RN, Rothman N (1999) Well-done, grilled red meat increases the risk of colorectal adenomas. *Cancer Res* 59(17):4320–4324
11. Sugimura T, Wakabayashi K, Nakagama H, Nagao M (2004) Heterocyclic amines: mutagens/carcinogens produced during cooking of meat and fish. *Cancer Sci* 95(4):290–299
12. Augustsson K, Skog K, Jagerstad M, Dickman PW, Steineck G (1999) Dietary heterocyclic amines and cancer of the colon,

- rectum, bladder, and kidney: a population-based study. *Lancet* 353(9154):703–707
13. Johnson RL, Fleet JC (2013) Animal models of colorectal cancer. *Cancer Metastasis Rev* 32(1–2):39–61
  14. Rosenberg DW, Giardina C, Tanaka T (2009) Mouse models for the study of colon carcinogenesis. *Carcinogenesis* 30(2):183–196
  15. Lynch HT (1986) Frequency of hereditary nonpolyposis colorectal carcinoma (Lynch syndromes I and II). *Gastroenterology* 90(2):486–489
  16. Miyoshi Y, Ando H, Nagase H, Nishisho I, Horii A (1992) Germ-line mutations of the APC gene in 53 familial adenomatous polyposis patients. *Proc Natl Acad Sci USA* 89(10):4452–4456
  17. Chambers WM, Warren BF, Jewell DP, Mortensen N (2005) Cancer surveillance in ulcerative colitis. *Br J Surg* 92(8):928–936
  18. Huxley RR, Ansary-Moghaddam A, Clifton P, Czernichow S, Parr CL, Woodward M (2009) The impact of dietary and lifestyle risk factors on risk of colorectal cancer: a quantitative overview of the epidemiological evidence. *Int J Cancer* 125(1):171–180
  19. Larsson SC, Rafter J, Holmberg L, Bergkvist L, Wolk A (2005) Red meat consumption and risk of cancers of the proximal colon, distal colon and rectum: the Swedish mammography cohort. *Int J Cancer* 113(5):829–834
  20. Slattery ML (2000) Diet, lifestyle, and colon cancer. *Semin Gastrointest Dis* 11(3):142–146
  21. Eckburg PB, Bik EM, Bernstein CN, Purdom E, Dethlefsen L (2005) Diversity of the human intestinal microbial flora. *Science* 308(308):1635–1638
  22. Louis P, Hold GL, Flint HJ (2014) The gut microbiota, bacterial metabolites and colorectal cancer. *Nat Rev Microbiol* 12(10):661–672
  23. Sleeth ML, Thompson EL, Ford HE, Zac-Varghese SEK, Frost G (2010) Free fatty acid receptor 2 and nutrient sensing: a proposed role for fibre, fermentable carbohydrates and short-chain fatty acids in appetite regulation. *Nutr Res Rev* 23(1):135–145
  24. Muhammad N, Steele R, Isbell TS, Philips N, Ray RB (2017) Bitter melon extract inhibits breast cancer growth in preclinical model by inducing autophagic cell death. *Oncotarget* 8(39):66226
  25. Azadeh H, Amir G, Vahid S, Razihi R, Hassan A (2014) Effects of  $\beta$ -sitosterol oral administration on the proliferation and differentiation of neural stem cells. *J Funct Foods* 8:252–258
  26. Wang M, Ma H, Tian C, Liu S, Ye X, Zhou D, Li Y, Hui N, Li X (2017) Bioassay-guided isolation of glycoprotein SPG-56 from sweet potato Zhongshu-1 and its anti-colon cancer activity in vitro and in vivo. *J Funct Foods* 35:315–324
  27. He K, Hu Y, Ma H, Zou Z, Xiao Y, Yang Y, Feng M, Li X, Ye X (2016) Rhizoma *Coptidis* alkaloids alleviate hyperlipidemia in B6 mice by modulating gut microbiota and bile acid pathways. *Biochim Biophys Acta* 1862(9):1696–1709
  28. Chen Y, Gao SG, Chen JM (2015) Serum CA242, CA199, CA125, CEA, and TSGF are biomarkers for the efficacy and prognosis of cryoablation in pancreatic cancer patients. *Cell Biochem Biophys* 71(3):1287–1291
  29. Engelman JA (2009) Targeting PI3K signalling in cancer: opportunities, challenges and limitations. *Nat Rev Cancer* 9(8):550–562
  30. Cantley LC (2002) The phosphoinositide 3-kinase pathway. *Science* 296(5573):1655–1657
  31. Jemal A, Bray F, Center MM, Ferlay J, Ward E, Forman D (2011) Global cancer statistics. *CA Cancer J Clin* 61(2):69–90
  32. Harris L, Fritsche H, Mennel R, Norton L, Ravdin P (2007) American society of clinical oncology 2007 update of recommendations for the use of tumor markers in breast cancer. *J Clin Oncol* 25(33):5287–5312
  33. Mayer IA, Arteaga CL (2015) The PI3K/AKT pathway as a target for cancer treatment. *Annu Rev Med* 67(1):11–28
  34. Engelman JA, Luo J, Cantley LC (2006) The evolution of phosphatidylinositol 3-kinases as regulators of growth and metabolism. *Nat Rev Genet* 7(8):606–619
  35. Salmela L, Carracedo A, Pandolfi PP (2008) Tenets of PTEN tumor suppression. *Cell* 133(3):403–414
  36. Manning BD, Cantley LC (2007) AKT/PKB signaling: navigating downstream. *Cell* 129(7):1261–1274
  37. Guertin DA, Sabatini DM (2007) Defining the role of mTOR in cancer. *Cancer Cell* 12(1):9–22
  38. Lu J, Fu L, Tang Z, Zhang C, Qin L, Wang J, Yu Z, Shi D, Xiao X, Xie F, Huang W, Deng W (2016) Melatonin inhibits AP-2 $\beta$ /hTERT, NF- $\kappa$ B/COX-2 and Akt/ERK and activates caspase/cyto C signaling to enhance the antitumor activity of berberine in lung cancer cells. *Oncotarget* 7(3):2985–3001
  39. Ahn J, Sinha R, Pei Z, Dominianni C, Wu J, Shi J, Goedert JJ, Hayes RB, Yang L (2013) Human gut microbiome and risk for colorectal cancer. *J Nat Cancer Inst* 105(24):1907–1911
  40. O’Keefe SJ (2008) Nutrition and colonic health: the critical role of the microbiota. *Curr Opin Gastroenterol* 24(1):51–58
  41. de Martel C, Ferlay J, Franceschi S, Vignat J, Bray F, Forman D, Plummer M (2012) Global burden of cancers attributable to infections in 2008: a review and synthetic analysis. *Lancet Oncol* 13(6):607–615
  42. Schwabe RF, Jobin C (2013) The microbiome and cancer. *Nat Rev Cancer* 13(11):800–812
  43. Elinav E, Nowarski R, Thaiss CA, Hu B, Jin C, Flavell RA (2013) Inflammation-induced cancer: crosstalk between tumours, immune cells and microorganisms. *Nat Rev Cancer* 13(11):759–771
  44. Irrazabal T, Belcheva A, Girardin SE, Martin A, Philpott DJ (2014) The multifaceted role of the intestinal microbiota in colon cancer. *Mol Cell* 54(2):309–320
  45. Garrett WS (2015) Cancer and the microbiota. *Science* 348(6230):80–86
  46. Sun F, Kong B, Chen Q, Han Q, Diao X (2016) N-nitrosoamine inhibition and quality preservation of Harbin dry sausages by inoculated with *Lactobacillus pentosus*, *Lactobacillus curvatus* and *Lactobacillus sake*. *Food Control* 73:1514–1521
  47. Bendali F, Kerdouche K, Hamma-Faradji S, Drider D (2017) In vitro and in vivo cholesterol lowering ability of *Lactobacillus pentosus* KF923750. *Benef Microbes* 8(2):271–280
  48. Kovatcheva-Datchary P, Arora T (2013) Nutrition, the gut microbiome and the metabolic syndrome. *Best Pract Res Clin Gastroenterol* 27(1):59–72
  49. Macfarlane GT, Macfarlane S (2012) Bacteria, colonic fermentation, and gastrointestinal health. *J AOAC Int* 95(1):50–60
  50. Clarke G, Stilling RM, Kennedy PJ, Stanton C, Cryan JF, Dinan TG (2014) Minireview: gut microbiota: the neglected endocrine organ. *Mol Endocrinol* 28(8):1221–1238
  51. Holzer P, Reichmann F, Farzi A (2012) Neuropeptide Y, peptide YY and pancreatic polypeptide in the gut-brain axis. *Neuropeptides* 46(6):261–274
  52. Baenke F, Peck B, Miess H, Schulze A (2013) Hooked on fat: the role of lipid synthesis in cancer metabolism and tumour development. *Dis Models Mech* 6(6):1353–1363